AUT Journal of Civil Engineering

AUT J. Civil Eng., 6(2) (2022) 191-204
DOI: 10.22060/ajce.2022.20830.5781

Investigation Progressive Collapse of K-Model Steel Truss Bridge under Additional Live Load Following Bridge Repairs

S. S. Jorfi[1], F. A. Gandomkar[2]*

[1] Civil Engineering Department, ACECR Institute of Higher Education, Khuzestan, Iran.
[2] Department of Structure, Faculty of Civil Engineering, Jundi-Shapur University of Technology, Dezful, Iran.

ABSTRACT: The main purpose of this study is to investigate the progressive collapse of the K-truss Bridge under additional live load caused by bridge repairs. In this case, the effect of several parameters such as length of members, bridge span ratio, steel grade, and load cases, were evaluated. The initial design of the bridge models was carried out using AASHTO LRFD Bridge Design Specifications. Bridge models were constructed with two different span ratios: bridge Model A with a common ratio of 1:2:1, and bridge Model B with a 1:1.3:1 span ratio. The results were obtained by a numerical finite element method using SAP2000 software. Results showed that the 1:1.3:1 span ratio is a more reasonable ratio for K-truss bridges. In all conditions, models with a span ratio of 1:1.3:1 had higher ultimate strength and more bearing capacity. In all load cases, models with a member length of 6m and a total height of 12m reduced the load-bearing capacity before reaching the yield displacement. Different lengths were provided for horizontal and vertical members of the trusses. Models with four-meter lengths had a higher bearing capacity than the three and six-meter models. The collapse process was different depending on the model details. All bridge models collapsed due to the buckling of the compression members.

Review History:

Received: Nov. 28, 2021
Revised: Nov. 05, 2022
Accepted: Nov. 07, 2022
Available Online: Nov. 29, 2022

Keywords:

Progressive collapse
Steel bridge
K-Truss
Non-linear static analysis
Bridge repair load

1- Introduction

Progressive collapse is defined as the extent of damage or collapse that is disproportionate to the magnitude of the initiating event [1]. The repair processes require heavy materials and machinery, which may weigh many times more than the structural capacity. This type of loading is not considered in the design. In 2007, the collapse of the I-35w bridge in Minnesota, United States, was reported to be due to the multiplication of the load during the repair process [2, 3]. Miyachi *et al.* in 2012, studied the progressive collapse analysis of Warren steel truss bridges. They showed the collapse of the mentioned bridge happened because of buckling when some elements reached yield stress [4]. In 2016, Khuyen and Iwasaki presented an empirical equation to calculate the dynamic amplification factor (DAF) for alternate load path in redundancy and progressive collapse linear static analysis against the initial sudden member fracture. Allows to computation of DAF from the maximum norm stress σ_{is}/σ_{iy} in the static linear elastic analysis of the damaged model with a member removal [5]. Wolff and Starossek in 2009, studied the loss of cables and the progressive collapse of cable bridges. Considering the weakening of the cables and the transverse vibrations of the cables, bending anchors are created in some parts of the tower [6]. Cai *et al.* in 2012, compared the different methods of analyzing the progressive collapse of cable bridges. The dynamic reinforcement factor of 2 is a good estimate for the static analysis method because linear dynamic and linear static methods result in approximately the same maximum flexural deformation [7]. Aoki *et al.* in 2013, show that the nonlinearity of the materials has little effect on the progressive collapse response. If the critical damping ratio is within the acceptable range (2%), it can be said that the damping ratio has little effect on the dynamic, progressive collapse. Also, geometric nonlinearity has a limited effect on the progressive collapse response caused by the loss of cables for properly designed bridges (less than 7%) [8]. In 2013, Olmati and Giuliani examined the susceptibility of a long-span suspension bridge to progressive collapse and found that this type of bridge was not highly susceptible to progressive collapse. When five or six pendants are removed symmetrically, indirect damage to the deck begins on each side of the bridge, which appears likely to remain locally just below the pendant area [9]. Lu and Zhang in 2013, investigated the progressive collapse of the pile foundation of a bridge by a ship's impact and show that the base collapse of the bridge initiates by the impact of the ship from the joints of the columns and piles where the maximum bending anchor exceeds the bending capacity [10]. In 2014, Miao studied progressive collapse analysis based on the reliability of bridge systems. It was found that most studies of structural redundancy and progressive collapse are based on deterministic analysis methods [11]

*Corresponding author's email: farhad@jus.ac.ir

The City investigated the effect of dynamic loading of cables on the progressive failure collapse of cable bridges and find that the center of the bridge deck and the top of the towers are the most critical points in the cable bridge, and the end cables on each side of the bridge are the most vulnerable. Whatever the distance between the broken cables and towers is reduced, the possibility of a total structural collapse is reduced too [12]. Samali *et al.* in 2015, investigated the effect of loading pattern and deck geometry on the progressive collapse response of cable bridges. It is concluded that deck geometry has little effect on the progressive collapse response of cable bridges [13]. In 2015, Bi *et al.*, Conducted a case study of Domino-type progressive collapse analysis on the Hongqi Viaduct Multi-Span Bridge with simple support. Based on the Numerical results, the methods of reducing the possibility of progressive collapse were proposed. A simple analytical method was presented for collapse analysis [14]. In 2016, Miao and Ghosn developed a reliability-based method for performing probabilistic progressive collapse analysis and calibration of incremental analysis criteria in highway bridges. The proposed method can help bridge engineers to calibrate reliability-based metrics, perform traditional incremental analyzes, and determine the ability of the bridge system in reducing progressive collapse [15]. In 2016, Das *et al.* studied the progressive failure of cable bridges. The results show that the failure of the cable that is close to the towers reduced the probability of progressive collapse. End cables are the most vulnerable cables, and their failure increases the possibility of progressive collapse [16]. Wani and Talikoti in 2016, investigated the progressive collapse response of cable bridges to the flexural deformation and axial force of the cables. With the loss of cables, the axial force becomes unbalanced in the cables, which increases the risk of collision with moving loads. The shape of the deck has little effect on the dynamic response after the loss of one or two cables [17]. Scattarreggia *et al.* in 2021 used field observations and the results of applied element modeling to analyze the Caprigliola bridge collapse in Italy. They assess the most likely damage mechanism that intersected between observed and modeled scenarios. Also recommended intermixing regular monitoring and inspection as well as reliable structural modeling to outline the impending severities in bridges [18]. In 2020 CRESPI *et al.* presented an efficient procedure for the collapse mechanism evaluation of existing reinforced concrete motorway bridges under horizontal loads, considering the corrosion effects due to carbonation through a simplified model that takes into account the steel rebar reduction. The proposed procedure allows the identification of the first structural element that reaches the collapse. [19]. Peng *et al.* in 2020 examined a particular collapsed ramp bridge in the Xiaoshan District of Zhejiang Province in China by taking advantage of various incidental observations to infer the collapse process and causes. This case study shows that a proper fusion of pre-and post-event data can shed light on the overturning collapse mechanisms of box-girder bridges, and illuminates potential hazards in existing bridges with similar geometries [20]. Hu *et al.* in 2021 investigated the Florida International University pedestrian bridge in the United States as a two-span pre-stressed reinforced concrete bridge, which collapsed during its construction in March 2018. The force transmission path is relatively simple, leading to a massive change of the internal force of the other parts of the structure once a breakdown occurs in an individual link. [21]. In 2020, Ozcelik and Tutus investigated the actual cause of the collapse with recommendations for future projects. The Botan Bridge, built in Siirt Pervari district, was planned to be the country's longest free cantilever bridge before it collapsed. Accordingly, the construction stages of the free cantilever bridge should be predicted and computer model should be established. [22]. Bai *et al.* in 2021, studied the progressive collapse method (PCM) in ship structures, in which local buckling is simplified by average compressive stress-strain curves of stiffened plates, to analyze the ultimate bearing capacity of steel box girders for bridges. The ultimate bearing capacity is influenced by local buckling [23].

Previous research on the progressive collapse of bridges has investigated many types of bridges, while no study has been conducted on the progressive collapse of the K-model steel truss bridge under additional live load following bridge repairs. Therefore, the main purpose of the current research is to study the progressive collapse of the K-truss Bridge. This research clarifies the collapse process of the three-span steel K-truss bridge models with a total length of 240 m. Progressive collapse analysis carry out for five load cases on two bridge models with different span ratios investigated. The truss members' connections are considered direct and without a gusset plate. Non-linearity of materials and non-linear geometry are considered in the modeling. In addition, the effect of span ratio, length of the chord, usage of steel material properties, and live load distribution effects on the ductility of the bridge models are studied. The displacements and deformations are investigated in different cases. The ductility of the bridge models is calculated and compared using their yielding load.

2- Structural Models

The K-truss bridge model is assumed to have three spans with a total length of 240 meters. The width of the bridge considering two lanes, including pavement and turrets, is assumed 10.4 meters. The models are classified into two groups, Group A and Group B, to investigate the effect of the span ratio on the collapse process. Figs. 1 and 2 show the side view of the bridge models. The span ratio of Group A is 1:2:1, so the length is assumed 120 meters for mid-span and 60m for side spans. The span ratio of 1:1.3:1 is generally prevailing in the design of truss bridges used in Group B, so the length of the mid-span is 96 meters, and the length of both side spans is 72 meters.

The five load cases used in this study are presented in the following (Fig. 3):

Load case a: $P_D + P_{L1}$, dead load plus uniform live load along the bridge and concentrated live load in the center of the mid-span.

Load case b: $P_D + P_{L2}$, dead load plus uniform live

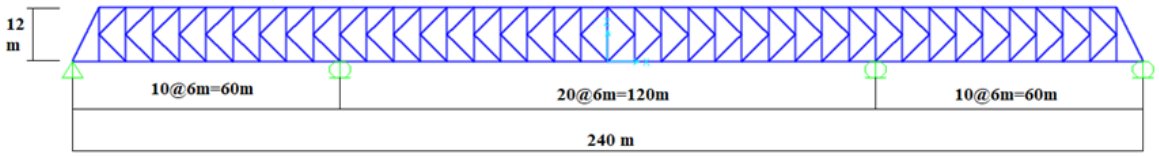

Fig. 1. Side View of Bridge: Model A.

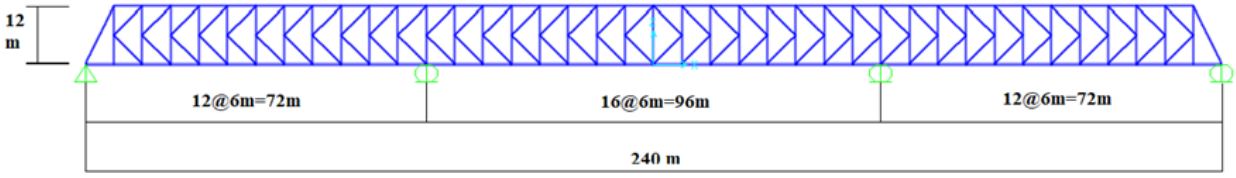

Fig. 2.Side View of Bridge: Model B.

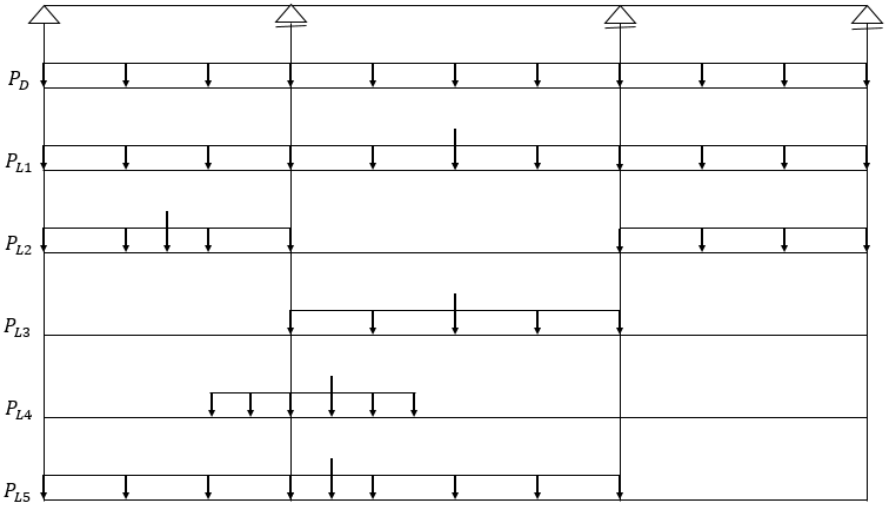

Fig. 3. Dead and Live Load Cases.

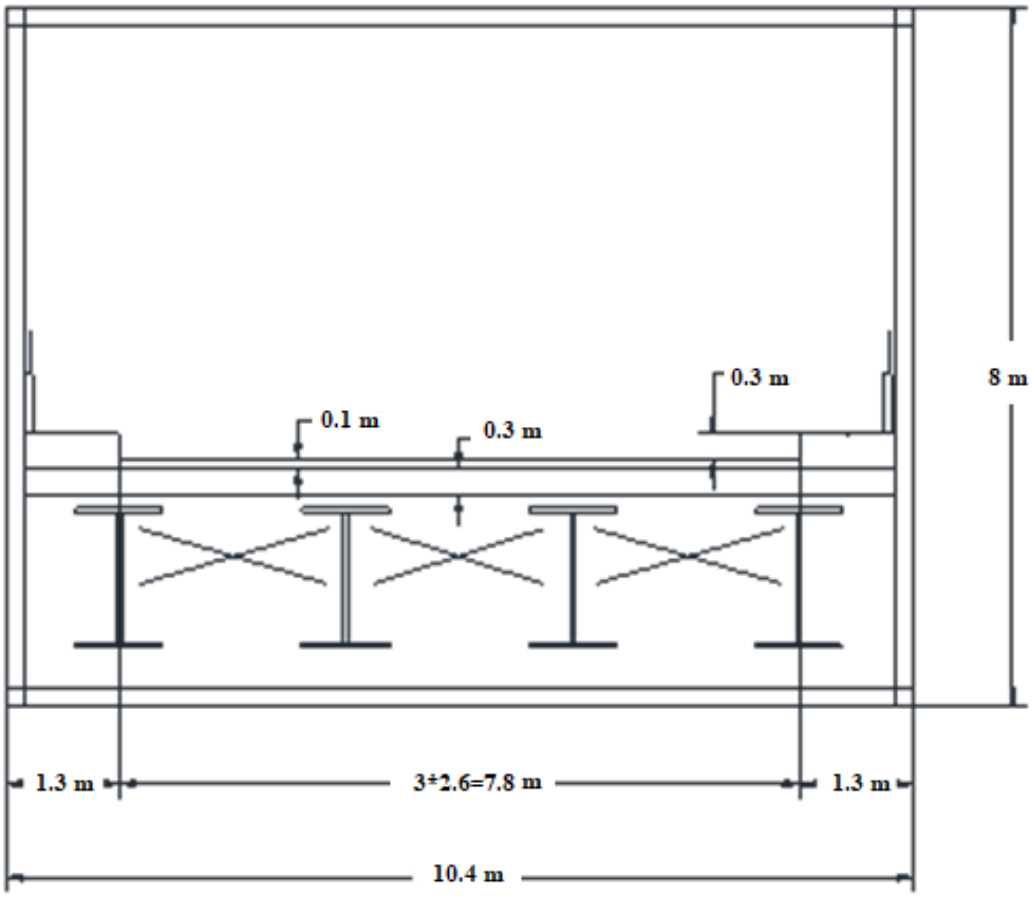

Fig. 4. Cross Section of Bridge Model.

load, applied on the side span of the bridge, and concentrated live load at the center of the side span,

Load case c: $P_D + P_{L3}$, dead load plus uniform live load applied on the mid-span and concentrated live load on the center of the mid-span.

Load case d: $P_D + P_{L4}$, dead load plus uniform live load distribution from the middle of the side span to the center of the bridge and concentrated live load applied near the support,

Load case e: $P_D + P_{L5}$, dead load plus uniform live load, applied on two adjacent spans to the center of the bridge, and concentrated live load applied near the support,

The lengths of the horizontal and vertical chords of the trusses were selected in the three sizes of 3, 4, and 6 meters to show the effect of the truss members' size on the collapse process. Fig. 4 shows the cross-section of the bridge model and deck system. RC slab is assumed for the bridge deck. The deck is made of reinforced concrete in addition to the asphalt surface. Sidewalk with a height of 0.4 meters from the asphalt surface of the deck on both sides. Four stringers are located 2.6 meters below the bridge deck. Two steel grades with different yield strengths (F_y) are used. The structural models studied in this paper are presented in Table 1.

3- Computational Model

Table 2 shows details of two steel grades used in this study [24]; ST52-3 with a tensile strength of 550 MPa and ST60-2 with 650 MPa. A reinforced concrete bridge deck is considered in the studied model. The AASHTO LRFD Bridge Design Specifications [25] code was employed for the preliminary design of the truss bridge. For simplification, the connections of the truss members were considered to be direct and without a gusset plate. The analytical approach is as follows. The dead load is applied first and then the live load is applied gradually until the bridge collapses. This can be expressed as $P_D + KP_L$ where K is the load increase coefficient. The analysis includes the elastic-plastic properties of steel and the large deformation effect. Truss design dead load is calculated at 96.96 kN/m. Based on Iranian code [26], design live loads are applied on the bridge with the amount of 14.67 kN/m and 156.91 kN as uniformly distributed and concentrated loads, respectively.

Initial design and analysis were done using SAP2000 software. The dead load was calculated using the mentioned details. The design live load adopted in this study is based on the Iranian Bridges Loading Regulations [26]. As shown in Fig. 3, five load cases, $P_D + P_{L1}$, $P_D + P_{L2}$, $P_D + P_{L3}$, $P_D + P_{L4}$ and $P_D + P_{L5}$ are considered in the analysis.

Table 1. Characteristics of Bridge Models.

Model No.	Span Ratio		$F_y\,(kN/m^2)$	Truss Members size (m)	h (m)	P_L
1	A	1:2:1	335000	3	6	P_{L1}
2		1:2:1	345000	3	6	P_{L1}
3		1:2:1	335000	3	6	P_{L2}
4		1:2:1	345000	3	6	P_{L2}
5		1:2:1	335000	3	6	P_{L3}
6		1:2:1	345000	3	6	P_{L3}
7		1:2:1	335000	3	6	P_{L4}
8		1:2:1	345000	3	6	P_{L4}
9		1:2:1	335000	3	6	P_{L5}
10		1:2:1	345000	3	6	P_{L5}
11		1:2:1	335000	4	8	P_{L1}
12		1:2:1	335000	4	8	P_{L2}
13		1:2:1	335000	4	8	P_{L3}
14		1:2:1	335000	4	8	P_{L4}
15		1:2:1	335000	4	8	P_{L5}
16		1:2:1	335000	6	12	P_{L1}
17		1:2:1	335000	6	12	P_{L2}
18		1:2:1	335000	6	12	P_{L3}
19		1:2:1	335000	6	12	P_{L4}
20		1:2:1	335000	6	12	P_{L5}
21	B	1:1.3:1	335000	3	6	P_{L1}
22		1:1.3:1	345000	3	6	P_{L1}
23		1:1.3:1	335000	3	6	P_{L2}
24		1:1.3:1	345000	3	6	P_{L2}
25		1:1.3:1	335000	3	6	P_{L3}
26		1:1.3:1	345000	3	6	P_{L3}
27		1:1.3:1	335000	3	6	P_{L4}
28		1:1.3:1	345000	3	6	P_{L4}
29		1:1.3:1	335000	3	6	P_{L5}
30		1:1.3:1	345000	3	6	P_{L5}
31		1:1.3:1	335000	4	8	P_{L1}
32		1:1.3:1	335000	4	8	P_{L2}
33		1:1.3:1	335000	4	8	P_{L3}
34		1:1.3:1	335000	4	8	P_{L4}
35		1:1.3:1	335000	4	8	P_{L5}
36		1:1.3:1	335000	6	12	P_{L1}
37		1:1.3:1	335000	6	12	P_{L2}
38		1:1.3:1	335000	6	12	P_{L3}
39		1:1.3:1	335000	6	12	P_{L4}
40		1:1.3:1	335000	6	12	P_{L5}

Table 2. Mechanical Properties of Steel.

Steel Grade	ST60-2	ST52-3
Tensile Strength (N/mm^2)	$\sigma_u = 650$	$\sigma_u = 550$
Yield Stress (N/mm^2)	$\sigma_y = 335$	$\sigma_y = 345$
Yield Strain (%)	$\varepsilon_y = 0.1675$	$\varepsilon_y = 0.1725$
Elastic Modulus (N/mm^2)	$E = 2.0\times10^5$	$E = 2.0\times10^5$

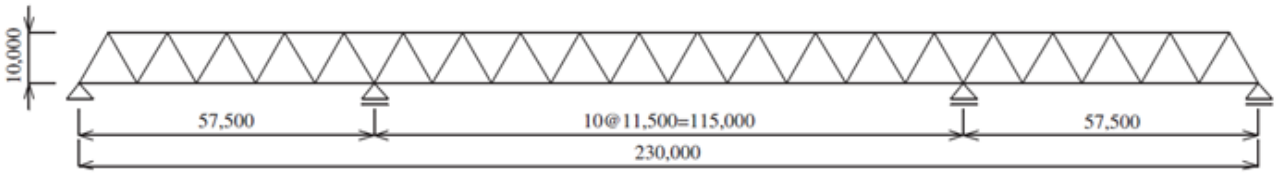

Fig. 5. Side View of Warren Bridge Model in Miyachi study (unit: mm) [4].

Dead and live loads are assumed to be fully loaded onto the deck and applied equally to both trusses. Two-dimensional models were used to perform the progressive collapse analysis, and the torsion effects were neglected. The live load increased following the full application of the dead load. This trend continues until the bridges collapse. Nonlinear static analysis was performed to explain the effect of the amount and distribution of the live load (Fig. 3) on the ultimate resistance of various truss members. The location of the concentrated live load was considered the critical point in the behavior of the structures.

Nonlinear buckling may be evaluated in SAP2000 using nonlinear static analysis. This procedure takes an iterative approach while implementing P-Delta and Large-Displacement effect. During Nonlinear-static buckling analysis, the total load is applied incrementally. Stiffness and response are evaluated at each increment. Between each displacement step, stiffness may change due to the P-Delta effect, which involves large tensile or compressive stresses on transverse bending and shear behavior, and also the Large-Displacement effect, in which deformed configuration is considered when assembling the equilibrium equations.

In the case of criteria of buckling and yielding of the member, plastic hinges are considered in appropriate situations of the member. Then compressive, tensile, and buckling capacities are assigned to the plastic hinges. After that during increasing load, which applies to the structural system, members with forces further than mentioned capacities are determined.

4- Results and Discussion

The relation between compressive stress and strain of buckled members is shown in Figs. 16 to 19 and Figs. 24 to 27. The results of comparing groups A and B show that Group B models can bear more substantial stresses before the bridge collapses in the same conditions. A comparison of the load-displacement curve (in all load cases except Case b) shows that Group B has a higher load-bearing capacity than Group A. In load Case b when the uniform live load is applied to the bridge side spans, and the central live load is applied in the middle of the side span, Group A has a higher load-bearing capacity, and Group B can bear larger displacement.

4- 1- Verification

The main objective of this study is to investigate the progressive collapse of K-steel truss bridges. The results of a study conducted by Miyachi *et al.* are compared with the results of the finite element method in SAP2000 software. Miyachi *et al.* investigated progressive collapse for a Warren model steel truss bridge (Fig. 5). A Warren Bridge was initially subjected to dead load and then continued under additional live load from zero to yield of the member. For verification purposes, all the parameters are assumed similar to the study of Miyachi and are subsequently modeled and analyzed in SAP2000 software. Figs. 6 and 7 show that the results of the nonlinear static analysis of both studies are similar. The

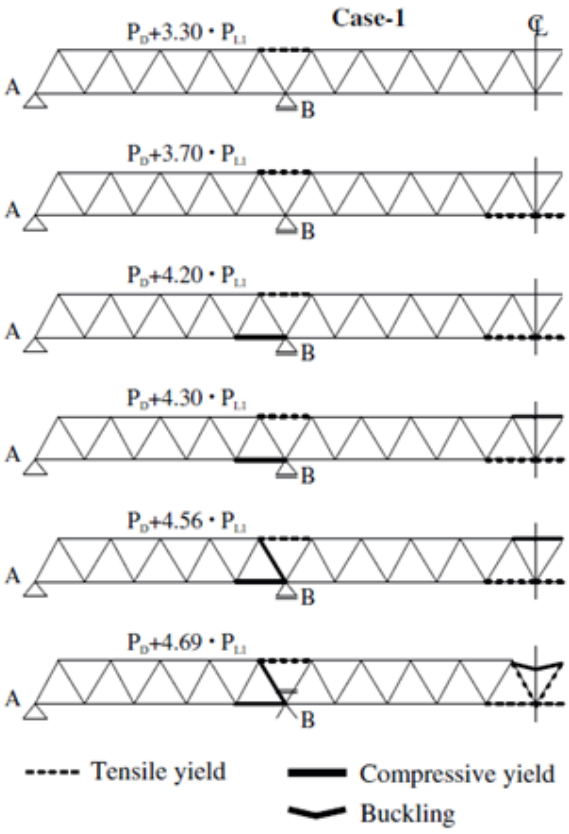

Fig. 6. Collapse process and final deformation of Bridge Model in Miyachi study [4].

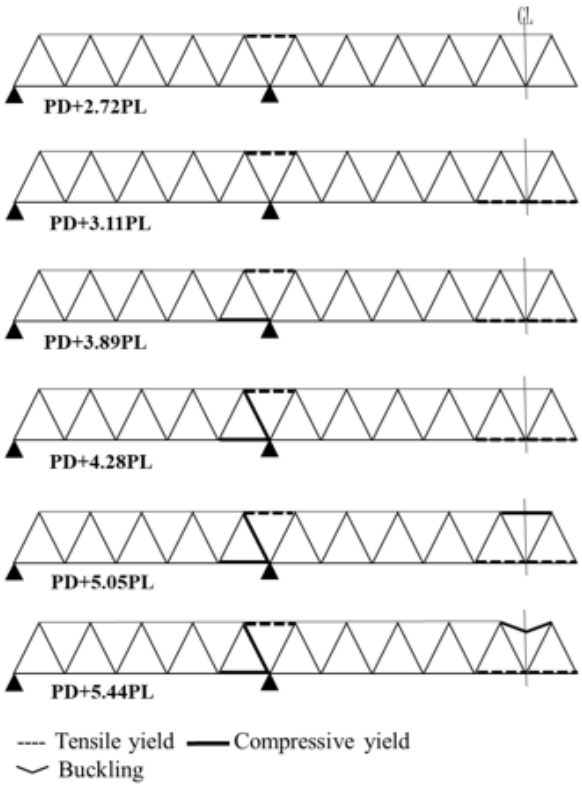

Fig. 7. Collapse process and final deformation of the current study.

Table 3. Percentage error of verification model.

Live load coefficients in the current study	Live load coefficients in the Miyachi study [4]	percentage error
2.90	3.30	12.06
3.33	3.70	9.86
4.03	4.20	4.02
4.28	4.30	0.37
4.18	4.56	8.31
4.22	4.69	10.07

comparison shows that the yielded points (compressive or tensile) in the present study and the Miyachi study both occur at the same location.

Table 3 compares the live load coefficients of the assumed model. A comparison of results and structure behavior in the SAP2000 model is in good agreement with the Miyachi study; hence, it is used as a foundation for constructing other research models.

4- 2- Obtained Results

In this study, progressive collapse analysis was carried out for a three-span continuous K-truss bridge with a total span length of 240 m in two different span ratios and five different live load distributions. The collapse process is clarified by the large deformation elastic-plastic method. The collapse process is different depending on the live load distribution and length of each span. It is aimed to clarify the collapse process, the collapse load, and the final deformation, and how the span ratio and the live load distribution affect the truss bridge load barring capacity.

4- 2- 1- Effect of size of truss members on progressive collapse

The vertical and horizontal length members of the

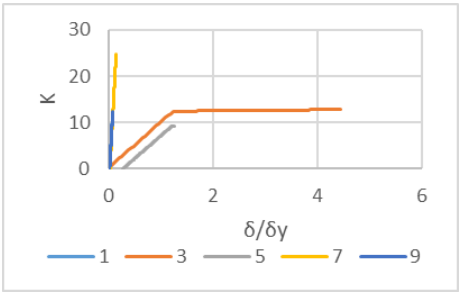

Fig. 8. Live Load Amplification Coefficient and Deflection of Bridge Model.

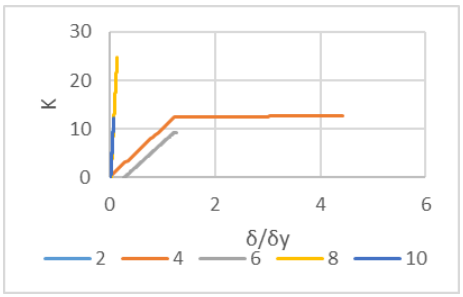

Fig. 9. Live Load Amplification Coefficient and Deflection of Bridge Model.

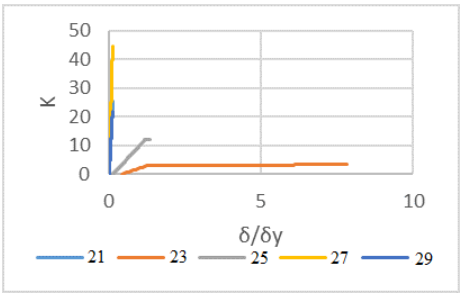

Fig. 10. Live Load Amplification Coefficient and Deflection of Bridge Model.

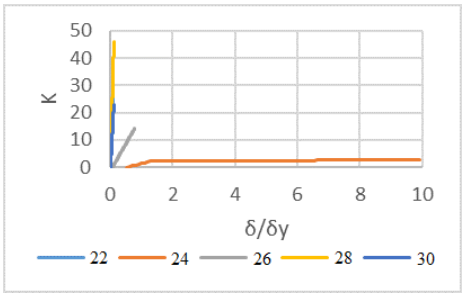

Fig. 11. Live Load Amplification Coefficient and Deflection of Bridge Model.

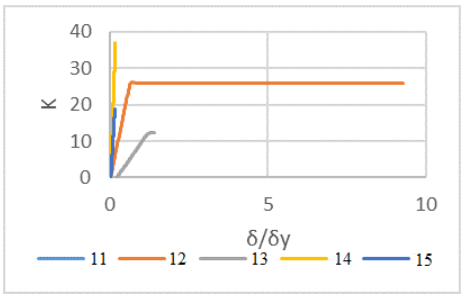

Fig. 12. Live Load Amplification Coefficient and Deflection of Bridge Model.

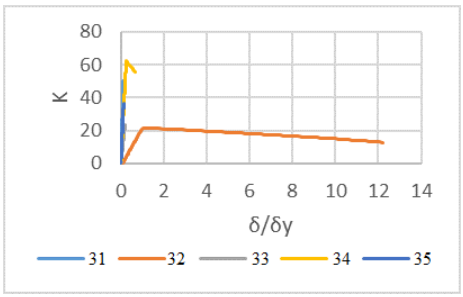

Fig. 13. Live Load Amplification Coefficient and Deflection of Bridge Model.

trusses are 3m, 4m, and 6m in different models. Figs. 8 to 15 illustrate the relationship between applied loads and vertical displacements at critical points in the structure. The horizontal axis represents the ratio of displacements to yield displacements and uses the live load factor rather than the actual load value in the vertical axis. In all loading cases, as the load increases, the displacement of the structure increases. The highest load-bearing capacity is associated with loading case "d" where the concentrated live load extends near the support, and the uniform live load extends on the middle crater to the center of the structure. Given that in all models and all loading cases, the ultimate value of the live load coefficient K is higher than the calculated value in the design indicating that the designed bridges have a high degree of safety against live loads.

In the bridge with a 3m member length, in Case b where the uniform live load is applied at the bridge side spans and the concentrated live load at the middle of the side span, and the Case c where the uniform live load is applied at the middle span and the concentered live load is applied at the same span, the structure loses its load-bearing capacity when reaching its yield displacement so that the load increases with

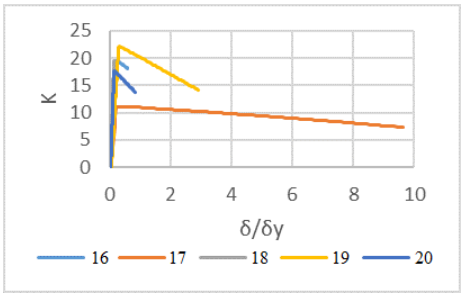

Fig. 14. Live Load Amplification Coefficient and Deflection of Bridge Model.

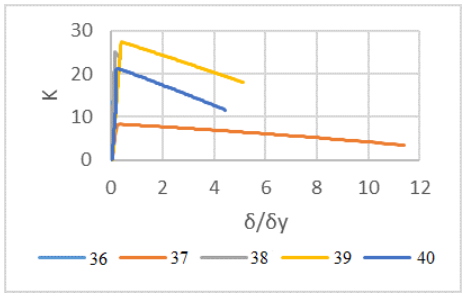

Fig. 15. Live Load Amplification Coefficient and Deflection of Bridge Model.

minimal slope. Whereas in loading of cases a, d, and e, the structure collapses before reaching its yield displacement.

The maximum load-bearing capacity in the bridge with a 4m member length is higher than the bridge with a 3m and 6m member length. This shows that in the same conditions, a truss with a 4m member length will perform better than the trusses with a 3m and 6m member length. In all load cases, the bridge with a 6m member length and a total height of 12m, reduce the load-bearing capacity of the structure before reaching the yield displacement. The results show the truss bridge collapsed because of buckling after it reaches the yield stress in all cases and did not depend on the size of the truss members. The collapse of the truss is caused by the destruction of local failure. So structural strength analysis is crucial for designing collapse strength.

4- 2- 2- Effect of steel grade on progressive collapse

Two groups are defined based on their steel grade, the ST60-2 group, $F_y = 335000(kN/m^2)$, and the ST52-3 group, $F_y = 345000(kN/m^2)$. Examining the live-displacement and the stress-strain curves in different states shows that the influence of the steel grade on structural performance is negligible.

4- 2- 3- Effect of live load case on progressive collapse

Five different load cases were considered for the uniform and concentrated live loads. The details of the load cases are described in the preceding sections (Fig. 3). The load-displacement curve shows that under different load cases and in the same conditions, Group B has a higher load-bearing capacity than Group A. Only in Case of b when the uniform live load is applied to the side spans and the concentrated live load is applied in the middle of the side span, the Group A models have the higher load-bearing capacity. Group B can bear greater displacement (Figs. 8 to 15). The coordination of the stress-strain diagram and its variations in the tensile and compressive yield members show that different load cases (a, b, c, d, and e) do not affect the stress-strain changes. Although the value of additional live load due to the maintenance process, which led to the buckling of the truss member cannot be determined, this buckling is the key to the collapse of the entire bridge. Summarized results in all cases show bridge models collapse because of compression buckling members.

4- 2- 4- Effect of span ratio on progressive collapse

To investigate the effect of the location of the bridge supports on the collapse process, the models are classified into two groups, Group A and Group B. The span ratio in Group A was assumed to be 1:2:1, so the mid-span length is 120 m, and the side spans are 60 m. In Group B, the ratio of 1:1.3:1 is maintained so that the mid-span and side spans are 96 and 72 m, respectively. The results of comparing Group A models 1 to 20 and Group B models 21 to 40 in members subjected to compressive yield show that in the same conditions, Group B models can carry higher stresses before the structure collapse.

The maximum strain in members with tensile yields is about 0.006 and 0.024 for models with 3 and 4 m members, respectively. For models with 6-m members with a 1:2:1 span length ratio, Group A has a maximum tolerable compressive strain of 0.05, and for Group B, is about 0.024. The maximum compressive strain tolerances for models with 3m and 4m members are about 0.006 and 0.024, respectively. For models with 6-m members with a 1:2:1 span length ratio, Group A has a maximum tolerable compressive strain of 0.05, and for Group B is about 0.024. The coordination of the stress-strain diagram and its variations in the tensile and compressive members show that different loading modes (a, b, c, d, and e) do not affect the stress-strain changes. The maximum strain of a tensile member in all cases is less than 10%. So, it is concluded that bridge models do not collapse due to fracture of tensile members, but due to buckling of compressive members.

5- Ductility

In this section, the ductility of the bridge models is computed and evaluated by defining K_y as the live load coefficient when the first member yields and K_u as the live load coefficient when the live load increment and buckling occurs. The ductility index obtained by the fraction of the coefficient K_u over K_y for each model is provided in the following tables. Given the values of μ in almost all cases, the values of the ductility coefficient in Group A are higher than those in Group B, so it can be said that the models in Group A with the span ratio of 1:2:1 are more flexible.

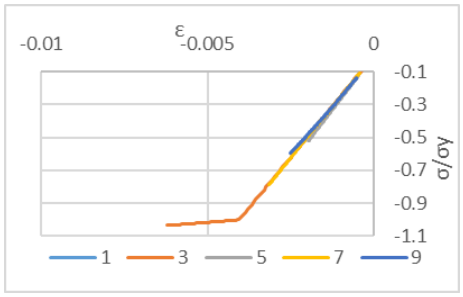

Fig. 16. Compressive Stress-Strain of Bridge Model.

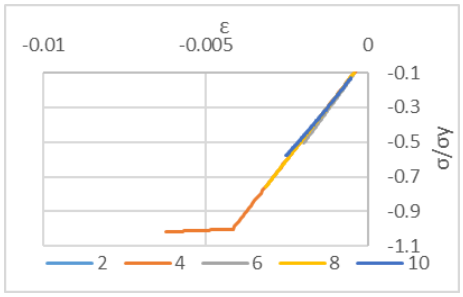

Fig. 17. Compressive Stress-Strain of Bridge Model.

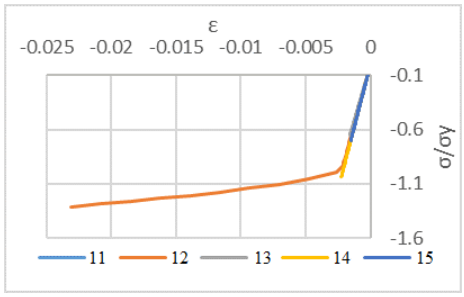

Fig. 18. Compressive Stress-Strain of Bridge Model.

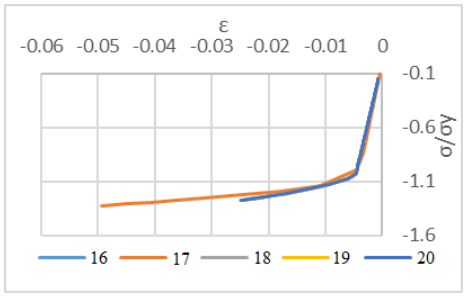

Fig. 19. Compressive Stress-Strain of Bridge Model.

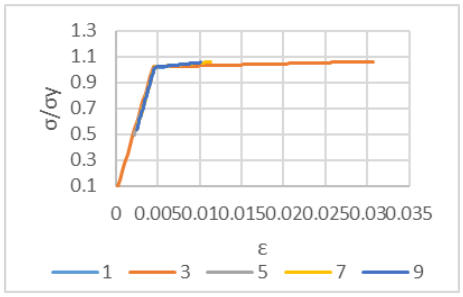

Fig. 20. Tensile Stress-Strain of Bridge Model.

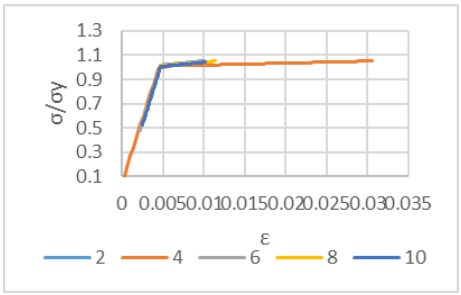

Fig. 21. Tensile Stress-Strain of Bridge Model.

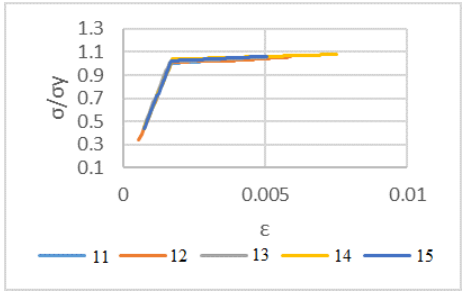

Fig. 22. Tensile Stress-Strain of Bridge Model.

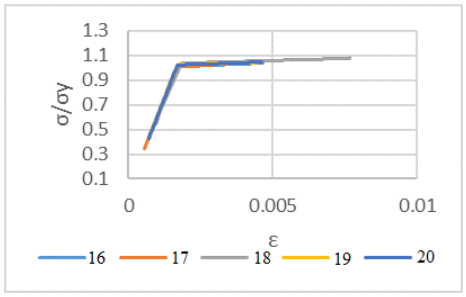

Fig. 23. Tensile Stress-Strain of Bridge Model.

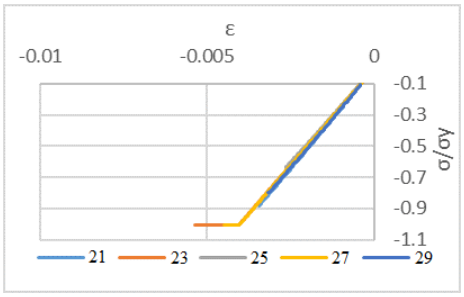

Fig. 24. Compressive Stress-Strain of Bridge Model

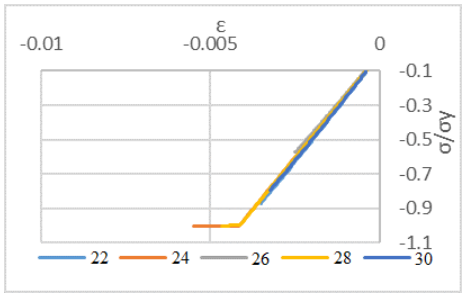

Fig. 25. Compressive Stress-Strain of Bridge Model

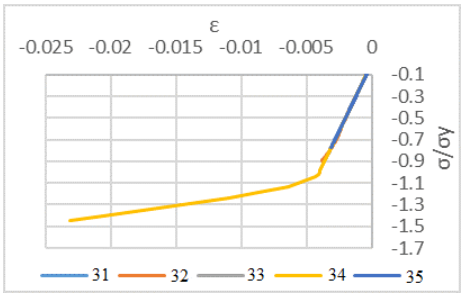

Fig. 26. Compressive Stress-Strain of Bridge Model

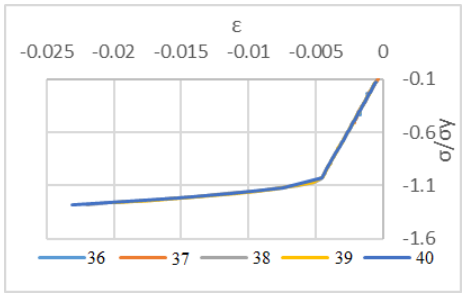

Fig. 27. Compressive Stress-Strain of Bridge Model

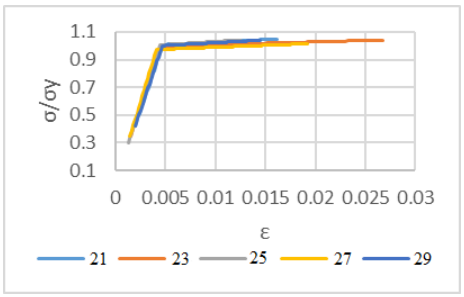

Fig. 28. Tensile Stress-Strain of Bridge Model.

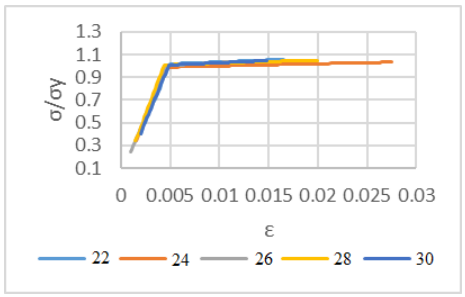

Fig. 29. Tensile Stress-Strain of Bridge Model.

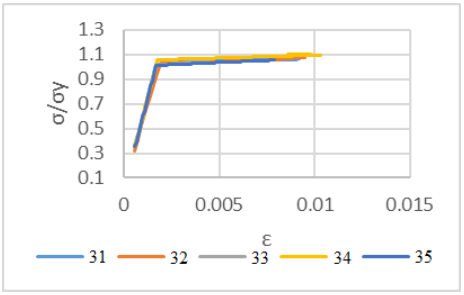

Fig. 30. Tensile Stress-Strain of Bridge Model.

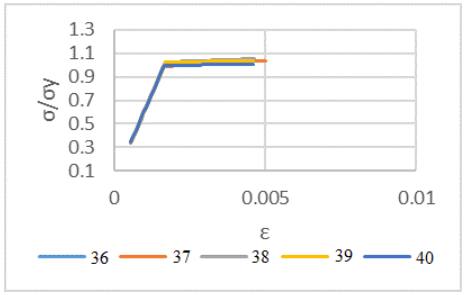

Fig. 31. Tensile Stress-Strain of Bridge Model.

Table 4. Ductility of Bridge: Model A.

Model No.	K_y	K_u	$\mu = K_u / K_y$
1	2.624515	2.982007	1.136213
2	2.862854	3.220283	1.124851
3	6.639808	7.082395	1.066657
4	6.639808	7.082395	1.066657
5	2.802784	3.092628	1.103413
6	2.996015	3.189239	1.064494
7	4.221629	4.718297	1.117648
8	4.718297	4.966631	1.052632
9	2.724451	3.095483	1.136186
10	2.971819	3.095483	1.041612
11	3.591631	3.950671	1.099966
12	7.230584	7.230584	1
13	3.151611	3.451568	1.095176
14	4.082049	4.453066	1.09089
15	3.216178	3.594534	1.117641
16	2.68766	3.17606	1.181719
17	5.580947	5.580947	1
18	2.844849	3.063593	1.076891
19	3.139253	3.662278	1.166608
20	2.39773	2.93042	1.222164

6- Conclusion

In this study, progressive collapse analysis is carried out on a three-span continuous K-truss bridge with a total length of 240m. Five different live load distributions are considered for two bridge models with different span ratios. A large deformation elastic-plastic method is used to show the collapse process. Various factors affect the process of bridge collapses. In this course, collapse load, final deformation, and stress-strain diagram are investigated. The ductility of the bridges was calculated using the live load coefficient and the effect of span ratio on ductility was compared. Examining the stress-strain curves in members that observe tensile or compressive yields shows that, in all models, an increase in tension (tensile or compressive) in the members causes an increase in strain, and after reaching the yield stress, changes in strain continue with a minimal slope. The maximum strain of a tensile member in all cases is less than 10%. So, it is concluded that bridge models did not collapse due to fracture of tensile members, but due to buckling of compressive members. It is common in both steel grades that changing the steel grade from ST52 to ST60 did not make much difference in the results. The graphs of live load coefficients at the different load cases show that the influence of steel type on structural performance is negligible. Load-displacement diagrams show that models constructed with vertical and horizontal members, 4m in length and 8m in height, can carry more loads than trusses constructed with members of 3m and 6m in length. The maximum load-bearing capacity is associated with loading case “d” where the concentrated live load extends near the support, and the uniform live load is distributed from the middle crater to the center of the structure which can reach multiple times the design capacity. All bridge models collapse due to the buckling of compression members. Calculating the ductility coefficient for the other models and comparing them shows that the ductility coefficient values in Group A models are 1:2:1 higher than those in Group B with a 1:1.3:1 ratio. While models with a span ratio of 1:1.3:1 have higher ultimate strength and more bearing capacity. This suggests that the 1:1.3:1 ratio for the K-model truss bridges is more reasonable. Analytical results show the ultimate bearing

Table 5. Ductility of Bridge: Model B.

Model No.	K_y	K_u	$\mu = K_u / K_y$
21	4.347828	4.859321	0.89474
22	4.763452	5.028096	0.947367
23	2.923692	2.928692	0.998293
24	2.223749	2.228749	0.997757
25	3.969931	4.243502	0.935532
26	4.961833	5.245051	0.946003
27	6.234602	6.680006	0.933323
28	6.45966	6.921138	0.933323
29	4.179916	4.619719	0.904799
30	4.559801	5.015599	0.909124
31	5.303715	5.68248	0.933345
32	4.888671	4.888671	1
33	5.127398	5.593068	0.916742
34	5.602455	6.302613	0.88891
35	4.589637	4.94271	0.928567
36	3.888872	4.320792	0.900037
37	3.483776	3.483776	1
38	4.209656	4.85702	0.866716
39	5.19264	5.19264	1
40	3.568015	4.013903	0.888914

capacity is affected by local buckling. This fact is clear that the steel truss bridge is the most vulnerable to buckling becomes, and the effect of defects on the truss members is the most important. The whole collapse process shows that local damage to the bridge eventually leads to overall collapse. Failure to consider the repair load in the design of bridges or the alternative load path for members in which there is a possibility of buckling can prevent such a serious accident from occurring.

The novelty of the present study is clarifying the collapse process, buckling strength, and effects of live load distribution, truss member length, and the span ratio on a K-model truss bridge.

References

[1] General Services Administration, Alternate path analysis and design guidelines for progressive collapse resistance, (2016).

[2] J. Widley, Bridge description and collapse, Nation Transportation Safety Board (NTSB) report, Board Meeting HWY07MH024.

[3] N.T.S. Board, Highway Accident Report, Collapse of I-35W highway bridge, Minneapolis, Minnesota 2008–916203, (2007).

[4] K. Miyachi, S. Nakamura, A. Manda, Progressive collapse analysis of steel truss bridges and evaluation of ductility, Journal of constructional steel research, 78 (2012) 192–200.

[5] H.T. Khuyen, E. Iwasaki, An approximate method of dynamic amplification factor for alternate load path in redundancy and progressive collapse linear static analysis for steel truss bridges, Case Studies in Structural Engineering, 6 (2016) 53–62.

[6] M. Wolff, U. Starossek, Cable loss and progressive collapse in cable-stayed bridges, Journal of Bridge Structures, 5(1) (2009) 17-28.

[7] J. Cai, Y. Xu, L. Zhuang, J. Feng, J. Zhang, Comparison of various procedures for progressive collapse analysis of cable-stayed bridges, Journal of Zhejiang University-SCIENCE A (Applied Physics & Engineering), 13(5)

(2012) 323-334.

[8] Y. Aoki, H. Valipour, B. Samali, A. Saleh, A study on potential progressive collapse responses of cable-stayed bridges, advances in structural engineering, 16 (4) (2013) 689-706.

[9] P. Olmati, L. Giuliani, Progressive collapse susceptibility of a long span suspension bridge, Structures Congress, ASCE (2013) 272-283.

[10] Y.E. Lu, L.M. Zhang, Progressive collapse of a drilled-shaft bridge foundation under vessel impact, Journal of Ocean Engineering, 66 (1) (2013) 101–112.

[11] F. Miao, Reliability-based progressive collapse and redundancy analysis of bridge systems, Ph.D. Thesis, The City University of New York, CUNY Academic Works, (2014).

[12] R. Das, A.D. Pandey, Soumya, M.J. Mahesh, P. Saini, S. Anvesh, Effect of dynamic unloading of cables in collapse progression through a cable stayed bridge, Asian Journal of Civil Engineering (BHRC), 17 (4) (2016) 397-416.

[13] B. Samali, Y. Aoki, A. Saleh, H. Valipour, Effect of loading pattern and deck configuration on the progressive collapse response of cable-stayed bridges, Australian Journal of Structural Engineering, 16 (1) (2015).

[14] K. Bi, W. Ren, P. Cheng, H. Hao, Domino-type progressive collapse analysis of a multi-span simply-supported bridge: A case study, Journal of Engineering Structures, 90 (2015) 172–182.

[15] F. Miao, M. Ghosn, Reliability-based progressive collapse analysis of highway bridges, Journal of Structural Safety, 63 (2016) 33–46.

[16] R. Das, A.D. Pandey, Soumya, M.J. Mahesh, P. Saini, S. Anvesh, Progressive collapse of a cable stayed bridge, Journal of Procedia Engineering, 144 (2016) 132–139.

[17] A. Wani, R.S. Talikoti, A study on progressive collapse response of cable-stayed bridges for deflection and axial force in cables, International Research Journal of Engineering and Technology (IRJET), 03 (05) (2016) 1840-1843.

[18] N. Scattarreggia, R. Salomone, M. Moratti, D. Malomo, R. Pinho, G.M. Calvi, Collapse analysis of the multi-span reinforced concrete arch bridge of Caprigliola-Italy, Engineering Structures, 251 (2022) 113375.

[19] P. Crespi, M. Zucca, M. Valente, On the collapse evaluation of existing RC bridges exposed to corrosion under horizontal loads, Engineering Failure Analysis, 116 (2020) 104727.

[20] W. Peng, Z. Tang, D. Wang, X. Cao, F. Dai, E. Taciroglu, A forensic investigation of the Xiaoshan ramp bridge collapse, Engineering Structures, 224 (2020) 111203.

[21] Y.C. Hu, Y.H. Tan, F. Xi, Failure assessment and virtual scenario reproduction of the progressive collapse of the FIU bridge, Engineering Structures, 227 (2021) 111423.

[22] M. Ozcelik, O. Tutus, An investigation on Botan bridge (Siirt–Turkey) collapse during construction, Structures, 25 (2020) 268-273.

[23] L. Bai, R. Shen, Q. Yan, L. Wang, R. Miao, Y. Zhao, Progressive-models method for evaluating interactive stability of steel box girders for bridges–extension of progressive collapse method in ship structures, Structures, (2021) 3848-3861.

[24] Steel Bridge Design Guidelines-Report No.395, Country Management and Planning Organization, (2007).

[25] AASHTO LRFD BRIDGE DESIGN SPECIFICATIONS, American Association of State Highway and Transportation Official, Seventh Edition, (2014).

[26] Bridges Loading Regulations-Report No.139, Country Management and Planning Organization, (2000).

HOW TO CITE THIS ARTICLE

S. S. Jorfi, F. A. Gandomkar, Investigation Progressive Collapse of K-Model Steel Truss Bridge under Additional Live Load Following Bridge Repairs, AUT J. Civil Eng., 6(2) (2022) 191-204.

DOI: 10.22060/ajce.2022.20830.5781